

REPORT DOCUMENTATION PAGE				Form Approved OMB No. 0704-0188	
Public reporting burden for this collection of information is estimated to average 1 hour per response, including the time for reviewing instructions, searching existing data sources, gathering and maintaining the data needed, and completing and reviewing this collection of information. Send comments regarding this burden estimate or any other aspect of this collection of information, including suggestions for reducing this burden to Department of Defense, Washington Headquarters Services, Directorate for Information Operations and Reports (0704-0188), 1215 Jefferson Davis Highway, Suite 1204, Arlington, VA 22202-4302. Respondents should be aware that notwithstanding any other provision of law, no person shall be subject to any penalty for failing to comply with a collection of information if it does not display a currently valid OMB control number. PLEASE DO NOT RETURN YOUR FORM TO THE ABOVE ADDRESS.					
1. REPORT DATE (DD-MM-YY) 30/07/2008		2. REPORT TYPE Interim Report POSTPRINT		3. DATES COVERED (From - To) 30/07/2008	
4. TITLE AND SUBTITLE Many-body effects on optical carrier cooling in intrinsic semiconductors at low lattice temperatures				5a. CONTRACT NUMBER	
				5b. GRANT NUMBER	
				5c. PROGRAM ELEMENT NUMBER 61102F	
6. AUTHOR(S) Danhong Huang and P.M. Alsing				5d. PROJECT NUMBER 2304	
				5e. TASK NUMBER CR	
				5f. WORK UNIT NUMBER A1	
7. PERFORMING ORGANIZATION NAME(S) AND ADDRESS(ES) Air Force Research Laboratory Space Vehicles Directorate 3550 Aberdeen Ave., SE Kirtland AFB, NM 87117-5776				8. PERFORMING ORGANIZATION REPORT NUMBER AFRL-RV-PS-JA-2008-1004	
9. SPONSORING / MONITORING AGENCY NAME(S) AND ADDRESS(ES)				10. SPONSOR/MONITOR'S ACRONYM(S) AFRL/RVSS	
				11. SPONSOR/MONITOR'S REPORT NUMBER(S)	
12. DISTRIBUTION / AVAILABILITY STATEMENT Approved for public release; distribution is unlimited. (Clearance #RV08-261 – 10 Apr 08).					
13. SUPPLEMENTARY NOTES “Government Purpose Rights.” Interim Report for in-house DF621940. Published in the Physical Review B, Vol 78, p 035203 (2008).					
14. ABSTRACT Based on the coupled density and energy balance equations, a dynamical model is proposed for exploring many-body effects on optical carrier cooling (not lattice cooling) in steady state in comparison with the earlier findings of current-driven carrier cooling in doped semiconductors [X.L. Lei and C.S. Ting, Phys. Rev. B32, 1112 (1985)] and tunneling-driven carrier cooling through discrete levels of a quantum dot [H.L. Edwards et al., Phys. Rev. B52, 5714 (1995)]. This dynamical carrier-cooling process is mediated by a photoinduced nonthermal electron-hole composite plasma in an intrinsic semiconductor under a thermal contact with a low-temperature external heat bath, which is a generalization of the previous theory for a thermal electron-hole plasma [H. Haug and S. Schmitt-Rink, J. Opt. Soc. Am. B 2, 1135 (1985)]. The important roles played by the many-body effects such as band-gap renormalization, screening, and excitonic interaction are fully included and analyzed by calculating the optical-absorption coefficient, spontaneous emission spectrum, and thermal-energy exchange through carrier-phonon scattering. Both the optical carrier cooling and heating are found with increasing pump-laser intensity when the laser photon energy is set below and above the band gap of an intrinsic semiconductor. In addition, the switching from carrier cooling to carrier heating is predicted when the frequency detuning of a pump laser changes from below the band gap to above the band gap.					
15. SUBJECT TERMS SPACE VEHICLES;INFRARED;DETECTORS;QUANTUM WELL DETECTORS;SCATTERING IN SEMICONDUCTORS					
16. SECURITY CLASSIFICATION OF:			17. LIMITATION OF ABSTRACT Unlimited	18. NUMBER OF PAGES 9	19a. NAME OF RESPONSIBLE PERSON David Cardimona
a. REPORT Unclassified	b. ABSTRACT Unclassified	c. THIS PAGE Unclassified			19b. TELEPHONE NUMBER (include area code)

Many-body effects on optical carrier cooling in intrinsic semiconductors at low lattice temperatures

Danhong Huang and P. M. Alsing

Air Force Research Laboratory, Space Vehicle Directorate, Kirtland Air Force Base, New Mexico 87117, USA

(Received 4 April 2008; revised manuscript received 15 May 2008; published 11 July 2008)

Based on the coupled density and energy balance equations, a dynamical model is proposed for exploring many-body effects on optical carrier cooling (not lattice cooling) in steady state in comparison with the earlier findings of current-driven carrier cooling in doped semiconductors [X. L. Lei and C. S. Ting, *Phys. Rev. B* **32**, 1112 (1985)] and tunneling-driven carrier cooling through discrete levels of a quantum dot [H. L. Edwards *et al.*, *Phys. Rev. B* **52**, 5714 (1995)]. This dynamical carrier-cooling process is mediated by a photoinduced nonthermal electron-hole composite plasma in an intrinsic semiconductor under a thermal contact with a low-temperature external heat bath, which is a generalization of the previous theory for a thermal electron-hole plasma [H. Haug and S. Schmitt-Rink, *J. Opt. Soc. Am. B* **2**, 1135 (1985)]. The important roles played by the many-body effects such as band-gap renormalization, screening, and excitonic interaction are fully included and analyzed by calculating the optical-absorption coefficient, spontaneous emission spectrum, and thermal-energy exchange through carrier-phonon scattering. Both the optical carrier cooling and heating are found with increasing pump-laser intensity when the laser photon energy is set below and above the band gap of an intrinsic semiconductor. In addition, the switching from carrier cooling to carrier heating is predicted when the frequency detuning of a pump laser changes from below the band gap to above the band gap.

DOI: [10.1103/PhysRevB.78.035206](https://doi.org/10.1103/PhysRevB.78.035206)

PACS number(s): 73.21.Fg, 78.40.Fy, 78.55.Cr

I. INTRODUCTION

It is well known that the optical properties of an atomic vapor are essentially determined by the properties of a single atom in the linear-response regime,¹ i.e., a single-particle problem. However, the photoexcited electrons and holes inside an undoped semiconductor are quasiparticles moving freely throughout the whole crystal in the absence of lattice vibrations and structural defects. Therefore, the long-range characteristics of the Coulomb interaction between charged particles lead to a genuine many-body problem to determine optical properties of a semiconductor. The strong Coulomb interaction between electrons or between holes forces these charged quasiparticles to constitute a plasma, while the strong Coulomb interaction between an electron and a hole forces the pair to form an exciton. The many-body effects cause laser-intensity (or charge density which is proportional to the laser intensity) dependence of the optical spectra for semiconductors in the linear-response regime, i.e., the band-edge optical nonlinearity.²⁻⁴

When an n -doped semiconductor is under a bias field between two electrodes, free electrons in the semiconductor undergo a center-of-mass motion with a drift velocity.⁵ In this situation, free electrons reach a quasiequilibrium state with a resulting electron temperature due to an ultrafast relative scattering motion of electrons with themselves, with lattice ions and impurities. However, this electronic system usually does not stay in a thermal equilibrium with the lattice that has a different constant heat-bath temperature. Therefore, it is possible for drifting electrons to transfer their thermal energy to the lattice even when they are at a lower temperature than that of the lattice due to reduced phonon energy induced by a Doppler shift.⁵ As a result, electrical carrier cooling in steady state under a bias field is expected.

Another proposed approach for electrical carrier cooling involves using a tunneling band structure in quantum dots,⁶

in which hot electrons above the electron Fermi energy (or hot holes below the hole Fermi energy) are extracted using selective resonant tunneling through a discrete energy level of a quantum dot. This tunneling process modifies the quasiequilibrium carrier distribution function, leading to a sharpened step feature in a distribution (a downward step at the Fermi energy) with a lower temperature.

On the other hand, when an undoped semiconductor is subjected to a strong optical pumping, photogenerated electron-hole (e - h) plasmas are usually not in thermal equilibrium with a lattice having a fixed heat-bath temperature. This issue has not been addressed in the previous research,²⁻⁴ although it may be crucial for studying the saturation of optical absorption in undoped semiconductors under strong optical pumping. When an absorption saturation is reached in a steady state, there still exists an energy imbalance between the optically absorbed power and the power loss due to spontaneous emission of photons. Therefore, a dynamical energy equation is required to describe this energy imbalance and the compensation from the thermal exchange between phonons and photoexcited carriers.⁷ As a result, optical carrier cooling is expected in steady state with a pump laser if the optically absorbed power becomes smaller than the spontaneous power loss, which is different from the lattice cooling in semiconductors by photoluminescence. This turns out to be the microscopic origin for laser cooling of a lattice in thermally isolated semiconductors⁷⁻¹⁰ if the heating to the lattice such as Auger recombination¹¹ can be controlled in the system.

Carrier cooling and lattice cooling are physically different, although they may possess some mathematical similarities. The latter is a net cooling with a thermal isolation of the whole system from its environment, while the former is only a partial cooling of a system with a lower carrier temperature than the lattice temperature set by the thermal contact to an

external heat bath. In addition, the very difficult lattice cooling in semiconductors, if it exists, could be observed from the shift of the photoluminescence peak, while the easy carrier cooling can be directly verified by the delicate temperature dependence of the resonant tunneling current. Conceptually, slow lattice cooling with quasiequilibrium distributions of carriers and phonons, as well as an adiabatic variation of the lattice temperature, requires different carrier and lattice temperatures so that the thermal exchange between carriers and phonons becomes possible. Therefore, the basic assumption of equal temperatures in the papers by Rupper *et al.*¹² and by Sheik-Bahae *et al.*¹³ for both carriers and phonons cannot be applied to quasiequilibrium distributions of carriers and phonons.

In this paper, we will introduce the coupled dynamical density and energy balance equations to search appropriate laser photon energies and intensities for demonstrating the steady-state optical carrier cooling mediated by nonthermal electron-hole plasmas in an intrinsic semiconductor with a fixed lattice temperature set by an external heat bath. We will include many-body effects such as band-gap renormalization, screening, and excitonic interaction in calculating the optical-absorption coefficient, spontaneous-emission spectrum, and thermal-energy exchange through carrier-phonon scattering. By adjusting the laser photon energy above (below) the band-gap energy of an intrinsic semiconductor, we look for optical carrier heating (cooling) in the system. In addition, by sweeping the frequency detuning of a pump laser with respect to the band-gap energy, we expect to see a switching from optical carrier cooling to carrier heating.

The outline of this paper is as follows. In Sec. II, by employing the coupled dynamical density and energy balance equations, we present our model and theory to explore many-body effects on optical carrier cooling mediated by a nonthermal e - h composite plasma in intrinsic semiconductors. In Sec. III, we display and discuss numerical results for the optical carrier cooling as function of the laser intensity and photon energy, demonstrating the important role played by the many-body effect in the process of optical carrier cooling. A brief conclusion is given in Sec. IV with a remark.

II. MODEL AND THEORY

The ultrafast intraband electron-electron (hole-hole) scattering in an electron (hole) plasma ensures all electrons (holes) in a quasiequilibrium state with a time-dependent electron (hole) temperature $T_e(t)$ [$T_h(t)$] through an ultrafast thermalization process.¹⁴ Furthermore, the strong interband Coulomb interaction between the electron and hole plasmas locks their temperatures to the same value $T_c = T_e = T_h$ (Ref. 15). The lattice system is assumed in thermal contact with an external heat bath at a fixed temperature T_L . As a result, the phonons with a different temperature usually do not reach a thermal equilibrium with the charged carriers in the plasma.⁷

A. Dynamical density equation

The relative importance of various scattering processes in an undoped semiconductor depends on the type of materials

and the quality of material growth. For commonly used III-V materials such as GaAs, the growth processes are usually highly controlled, such that the density of crystal defects is low enough to become negligible. In this paper, we only consider the intrinsic properties of semiconductors for possible optical carrier cooling, i.e., $T_c < T_L$. Therefore, a defect-free crystal is assumed for the host semiconductor to be considered. Based on the conservation of number of electrons N_e and holes N_h per unit volume, the dynamical density equation that describes the temporal changes of the density $N_c = N_e = N_h$ of photoexcited carriers in intrinsic (defect-free and undoped) semiconductors under a spatially homogeneous laser illumination can be written as³

$$\frac{dN_c}{dt} = \frac{\beta_{\text{abs}}(\Omega_L)I_0}{\hbar\Omega_L} - \mathcal{R}_{\text{sp}}. \quad (1)$$

Here, $\hbar\Omega_L$ in Eq. (1) is the energy of incident photons, I_0 is the energy flux of the incident laser beam, $\beta_{\text{abs}}(\Omega_L)$ is the linear optical-absorption coefficient of the semiconductor, and \mathcal{R}_{sp} is the total rate of spontaneous emission of photons per unit volume. The three-body Auger recombination of excited e - h pairs,¹¹ which is proportional to the cube of N_c , has been neglected in Eq. (1) for low densities N_c and low laser intensity I_0 . The steady-state solution of Eq. (1) predicts a saturation of the optical absorption³ at early times when carriers are assumed to be in a thermal equilibrium with phonons, i.e., $T_c = T_L$. This equation can also be regarded as a generalization of the ABC rate model¹³ in the absence of Shockley-Reed-Hall nonradiative recombination¹⁶ and Auger recombination for defect-free semiconductors under low I_0 . For the temporal dependence, we assume that the incident field is turned on at time $t=0$. As a result, the initial condition for Eq. (1) is simply $N_c(0)=0$, where we have neglected the small intrinsic carrier density given by $n_i = \sqrt{\rho_c\rho_v} \times \exp(-E_G/2k_B T_c)$ with $\rho_c = 2(m_e^* k_B T_c / 2\pi\hbar^2)^{3/2}$ and $\rho_v = 2(m_h^* k_B T_c / 2\pi\hbar^2)^{3/2}$ due to $N_c \gg n_i$ at low temperatures. Here, m_e^* and m_h^* are the effective masses of electrons and holes, respectively, and E_G is the bare band-gap energy of the host semiconductor in the absence of photoexcited carriers. We will look for the steady-state solution of Eq. (1) in this paper.

1. Absorption coefficient

The frequency-dependent absorption coefficient in Eq. (1) is given by¹⁷

$$\beta_{\text{abs}}(\omega) = \beta_{\text{abs}}^{\text{pl}}(\omega) + \beta_{\text{abs}}^{\text{ex}}(\omega) = \frac{\omega\sqrt{\epsilon_b}}{n_r(\omega)c} \text{Im}[\alpha_L(\omega)], \quad (2)$$

where ϵ_b is the dielectric constant of the host semiconductor and $\alpha_L(\omega) = \alpha_L^{\text{pl}}(\omega) + \alpha_L^{\text{ex}}(\omega)$ is the total Lorentz function¹⁷ including contributions from both the e - h plasmas (denoted by the superscript pl), as well as from the excitons (denoted by the superscript ex). Here, the scaled refractive-index function in Eq. (2) is

$$n_r(\omega) = \frac{1}{\sqrt{2}} \{1 + \text{Re}[\alpha_L(\omega)] + \sqrt{[1 + \text{Re}[\alpha_L(\omega)]^2 + \{\text{Im}[\alpha_L(\omega)]\}^2}]^{1/2}\}. \quad (3)$$

The Lorentz function for the photoexcited e - h plasmas in the long-wavelength limit is calculated as^{3,18}

$$\alpha_L^{\text{pl}}(\omega) = -\frac{\Omega_{\text{pl}}^2}{\omega(\omega + i\gamma_0)} - \frac{2e^2}{\pi^2 \epsilon_0 \epsilon_b} \int_0^\infty dk k^2 |r_{\text{vc}}(k)|^2 [1 - f_e(k) - f_h(k)] \frac{E_e(k) + E_h(k)}{[\hbar(\omega + i\gamma_0)]^2 - [E_e(k) + E_h(k)]^2}, \quad (4)$$

where $\hbar\gamma_0$ is the homogeneous level broadening due to the finite lifetime of quasiparticles, k is the wave number of photoexcited carriers, and the plasma frequency of the e - h composite plasma in the first term of Eq. (4) is defined as

$$\Omega_{\text{pl}}^2 = \frac{N_c e^2}{\epsilon_0 \epsilon_b} \left(\frac{1}{m_e^*} + \frac{1}{m_h^*} \right) \equiv \frac{N_c e^2}{\epsilon_0 \epsilon_b \mu_r}, \quad (5)$$

where μ_r is the reduced e - h mass. In addition, the interband dipole-moment matrix element in the second term of Eq. (4) is

$$|r_{\text{vc}}(k)|^2 = \frac{E'_G}{4\mu_r} \frac{\hbar^2}{(E_G + \hbar^2 k^2 / 2\mu_r)^2}. \quad (6)$$

The kinetic energy $E_i(k)$ of quasiparticles for $i=e$ or h , initially introduced in Eq. (4), in the screened Hartree-Fock approximation is calculated as⁴

$$E_i(k) = \frac{E_G}{2} + \frac{\hbar^2 k^2}{2m_i^*} - \frac{e^2}{4\pi^2 \epsilon_0 \epsilon_b} \int_0^\infty dk' k'^2 f_i(k') \int_0^\pi d\theta \sin \theta \frac{1}{|\vec{k} - \vec{k}'|^2} \times \left[1 - \frac{\Omega_{\text{pl}}^2}{\omega_s^2(|\vec{k} - \vec{k}'|)} \right], \quad (7)$$

where $|\vec{k} - \vec{k}'| = \sqrt{k^2 + k'^2 - 2kk' \cos \theta}$, θ is the angle between \vec{k} and \vec{k}' , and the renormalized energy gap in Eq. (6) is given by $E'_G = E_e(0) + E_h(0)$. The last term in Eq. (7) includes the change in the exchange energy due to screening $\omega_s^2(q) = \Omega_{\text{pl}}^2(1 + q^2/q_s^2) + (\hbar q^2 / 4\mu_r)^2$ and the static screening length $1/q_s$ in the Thomas-Fermi limit is given by¹⁷

$$q_s^2 = \frac{e^2}{\pi^2 \epsilon_0 \epsilon_b k_B T_{c \ i=e,h}} \sum \int_0^\infty dk k^2 f_i(k) [1 - f_i(k)]. \quad (8)$$

The result in Eq. (7) includes the many-body energy renormalization effect, i.e., the reduction of the band-gap energy E_G with increasing carrier density or with decreasing carrier temperature. The distributions of photoexcited carriers, initially introduced in Eq. (4), are given by the following Fermi functions for $i=e$ and h :

$$f_i(k) = \left\{ \exp \left[\frac{E_i(k) - \mu_i}{k_B T_c} \right] + 1 \right\}^{-1}, \quad (9)$$

where μ_e and μ_h are the chemical potentials of electrons and holes. For given N_c and T_c at each moment, the chemical potential μ_i of carriers with $i=e$ and h is the root of the following equation:

$$\frac{1}{\pi^2} \int_0^\infty dk k^2 \left[\exp \left(\frac{E_i(k) - \mu_i}{k_B T_c} \right) + 1 \right]^{-1} - N_c = 0. \quad (10)$$

In Eq. (4), we show the Lorentz function for the photoexcited e - h plasmas. The Lorentz function for the s -type bound excitons is calculated as⁴

$$\alpha_L^{\text{ex}}(\omega) = -\frac{2e^2 \hbar^2}{\pi m_0^2 \epsilon_0 \epsilon_b a_B^3} |P_{\text{vc}}|^2 \sum_{n=1}^\infty \left[\frac{\eta_n}{(E'_G + E_n)n^3} \right] \times \frac{1 - f_e(0) - f_h(0)}{[\hbar(\omega + i\gamma'_0)]^2 - (E'_G + E_n)^2}, \quad (11)$$

where m_0 is the free-electron mass, γ'_0 is the dephasing rate of excitons, $n=1, 2, \dots$ is the radial quantum number of s -type bound excitons, $E_n < 0$ is the binding energy, and $a_B = 4\pi\epsilon_0\epsilon_b\hbar^2/\mu_r e^2$ is the effective Bohr radius. The interband-transition matrix element $|P_{\text{vc}}|^2$ in Eq. (11) for excitons is given by

$$|P_{\text{vc}}|^2 = \frac{m_0^2 E'_G}{4\mu_r}. \quad (12)$$

Moreover, we define η_n in Eq. (11) as the ratio given by

$$\eta_n = \frac{|\psi_n^{\text{ex}}(0)|^2}{|\phi_n^{\text{ex}}(0)|^2}, \quad (13)$$

where the exciton eigenfunctions $\psi_n^{\text{ex}}(r)$ and eigenenergies E_n in Eq. (11) are the solutions of the following Schrödinger equation for a screened exciton:

$$\frac{1}{r^2} \frac{d}{dr} \left[r^2 \frac{d\psi_n^{\text{ex}}(r)}{dr} \right] + \left\{ \frac{2\mu_r}{\hbar^2} \left[E_n + \frac{e^2}{4\pi\epsilon_0\epsilon_b r} \exp(-q_s r) \right] \right\} \psi_n^{\text{ex}}(r) = 0. \quad (14)$$

$\phi_n^{\text{ex}}(r)$ in Eq. (13) denotes the bare exciton eigenfunction with the binding energy $-E_B/n^2$ where $E_B = \hbar^2 / 2\mu_r a_B^2$. In addition, $\phi_n^{\text{ex}}(r)$ is also the solution of the above Schrödinger equation with $q_s=0$. The solution of Eq. (14) includes the many-body screening effect, i.e., E_n and η_n depend on q_s and decrease with increasing carrier density or carrier temperature. A more extensive treatment of nonlocal excitons has been proposed by Rupper *et al.*¹²

2. Spontaneous emission

The strong interaction of e - h plasmas with both incident and emitted photons forces the photon and charged carrier systems to stay in a thermal-equilibrium state, i.e., the same temperature for both photons and plasmas. In addition, we know that the radiative lifetime of photoexcited carriers in the host semiconductor is known to be on the order of 1–10 ns. If we work on a time scale slower than the radiative lifetime such as in a steady state, the statistics of the emitted

photons will obey the Bose-Einstein distribution at each moment with the same temperature as that of the carriers.³

Based on the assumption that charged carriers and photons have equal temperature T_c , the total rate of spontaneous emission per unit volume, $\mathcal{R}_{\text{sp}} = \mathcal{R}_{\text{sp}}^{\text{pl}} + \mathcal{R}_{\text{sp}}^{\text{ex}}$ in Eq. (1), can be related to the absorption coefficient $\beta_{\text{abs}}(\omega)$ through the so-called Kubo-Martin-Schwinger (KMS) relation.^{19–22} Our calculation includes the level broadening, which generalizes the KMS relation, and leads to²³

$$\begin{aligned} \mathcal{R}_{\text{sp}}^{\text{pl}} = & \left(\frac{\epsilon_b^{1/2} e^2}{\pi^5 c^3 \epsilon_0 \epsilon_b} \right) \int_0^\infty d\omega \omega^3 n_r(\omega) \theta(\hbar\omega - E'_G) \\ & \times \int_{E_h(0)}^{\hbar\omega - E_e(0)} d\xi f_e(\hbar\omega - \xi) f_h(\xi) \int_0^\infty dk k^2 |r_{\text{vc}}(k)|^2 \\ & \times \frac{\hbar^2 \gamma_0^2}{\{[\hbar\omega - \xi - E_e(k)]^2 + \hbar^2 \gamma_0'^2\} \{[\xi - E_h(k)]^2 + \hbar^2 \gamma_0'^2\}}, \end{aligned} \quad (15)$$

$$\begin{aligned} \mathcal{R}_{\text{sp}}^{\text{ex}} = & \left(\frac{\epsilon_b^{1/2} e^2 \hbar^2}{\pi^4 c^3 m_0^2 \epsilon_0 \epsilon_b a_B^3} \right) |P_{\text{vc}}|^2 \sum_{n=1}^\infty \left[\frac{\eta_n}{(E'_G + E_n)^2 n^3} \right] \int_0^\infty d\omega \omega^3 n_r(\omega) \theta(\hbar\omega - E'_G - E_n) \int_{E_h(0) + \lambda_h E_n}^{\hbar\omega - E_e(0) - \lambda_e E_n} d\xi f_e(\hbar\omega - \xi) f_h(\xi) \\ & \times \frac{\hbar^2 \gamma_0'^2}{\{[\hbar\omega - \xi - E_e(0) - \lambda_e E_n]^2 + \hbar^2 \gamma_0'^2\} \{[\xi - E_h(0) - \lambda_h E_n]^2 + \hbar^2 \gamma_0'^2\}}, \end{aligned} \quad (16)$$

where $\theta(x)$ is the step function, $\lambda_h = \mu_r/m_h^*$, $\lambda_e = \mu_r/m_e^*$, and $\lambda_e + \lambda_h = 1$. It is obvious from Eqs. (15) and (16) that \mathcal{R}_{sp} will be enhanced if N_c increases since it is proportional to $f_e f_h$. \mathcal{R}_{sp} could also be enhanced if E_G becomes large since it is proportional to ω^3 or E_G^3 .

B. Dynamical energy balance equation

It is known that the intraband carrier-carrier scattering time is on the order of 100 fs, which is much faster than the radiative lifetime of charged carriers. Therefore, the thermalization of hot carriers can be approximately regarded as an adiabatic process compared to the slow radiative-decay process, i.e., the total energy of charged particles remains conserved at each moment. Based on the conservation of total energy of charged particles, the dynamical energy equation for the e - h plasmas can be written as^{7,9}

$$C_0 \frac{dT_c}{dt} = \beta_{\text{abs}}(\Omega_L) I_0 - \mathcal{W}_{\text{sp}}(T_c) + \mathcal{W}_{\text{ph}}(T_c, T_L), \quad (17)$$

where the heat capacity of e - h plasmas is given by

$$C_0 = \frac{1}{2\pi^2 k_B T_c^2} \sum_{i=e,h} \int_0^\infty dk k^2 E_i(k) [E_i(k) - \mu_i] f_i(k) [1 - f_i(k)]. \quad (18)$$

We have introduced in Eq. (17) the power-loss density $\mathcal{W}_{\text{sp}} = \mathcal{W}_{\text{sp}}^{\text{pl}} + \mathcal{W}_{\text{sp}}^{\text{ex}}$ due to the spontaneous emission of photons. $\mathcal{W}_{\text{sp}}^{\text{pl}}$ and $\mathcal{W}_{\text{sp}}^{\text{ex}}$ in Eq. (17) are calculated by inserting the factor $\hbar\omega$ into Eqs. (15) and (16), respectively.

When both the defect and the Auger recombinations are neglected, the steady-state power condition can only be satisfied by including the thermal exchange between carriers and phonons as shown in Eq. (17). However, this important thermal exchange term has been dropped in the papers by Rupper *et al.*¹² and by Sheik-Bahae *et al.*¹³ when they used equal carrier and lattice temperature.

The initial condition for Eq. (17) is simply $T_c(0) = T_L$. In this paper, we will look for the steady-state solution of Eq. (17). Compared to the previous theory^{7,9} at earlier times, we have employed the generalized KMS relation in the calculations of $\mathcal{W}_{\text{sp}}^{\text{pl}}$ and $\mathcal{W}_{\text{sp}}^{\text{ex}}$. Because of the different lattice temperature T_L and carrier temperature T_c , there exists a thermal energy exchange between phonons and charged carriers in the system, which is represented by the last term on the right-hand side of Eq. (17) and is calculated by using the energy-dissipation theorem as⁹

$$\begin{aligned} \mathcal{W}_{\text{ph}}(T_c, T_L) = & \frac{\omega_{\text{LO}}}{2\pi^3} \left[n_{\text{ph}} \left(\frac{\hbar\omega_{\text{LO}}}{k_B T_L} \right) - n_{\text{ph}} \left(\frac{\hbar\omega_{\text{LO}}}{k_B T_c} \right) \right] \\ & \times \int_0^{q_m} q^2 dq |C_{q,\text{LO}}|^2 \int_0^\infty dk k^2 \int_0^\pi d\theta \sin \theta \\ & \times \sum_{i=e,h} [f_i(|\vec{k} + \vec{q}|) - f_i(k)] \delta[E_i(|\vec{k} + \vec{q}|) \\ & - E_i(k) + \hbar\omega_{\text{LO}}] + \frac{1}{2\pi^3} \sum_{\lambda=\text{LA,TA}} \frac{1}{\hbar^4 c_\lambda^3} \\ & \times \int_0^{\hbar\omega_m} dx x^3 |C_{q,\lambda}|^2 \left[n_{\text{ph}} \left(\frac{x}{k_B T_L} \right) - n_{\text{ph}} \left(\frac{x}{k_B T_c} \right) \right] \\ & \times \int_0^\infty dk k^2 \int_0^\pi d\theta \sin \theta \sum_{i=e,h} [f_i(|\vec{k} + \vec{q}|) - f_i(k)] \\ & \times \delta[E_i(|\vec{k} + \vec{q}|) - E_i(k) + x], \end{aligned} \quad (19)$$

where $|\vec{k} + \vec{q}| = (k^2 + q^2 + 2kq \cos \theta)^{1/2}$ and the photon-assisted phonon-scattering process⁷ is neglected for low I_0 . In Eq. (19), we assume the Bose function $n_{\text{ph}}(x) = 1/[\exp(x) - 1]$ for the phonon distribution, $\hbar\omega_{q\lambda}$ is the phonon energy for the wave number q and mode λ , and $|C_{q,\lambda}|^2$ represents the carrier-phonon coupling matrix element. For polar semicon-

ductors such as GaAs, there exist both acoustic and optical phonon modes.⁹ For optical phonon modes, only the longitudinal-optical phonon mode strongly couples to the charged carriers. Here, we set $\lambda = \text{LO, LA, and TA}$ representing longitudinal-optical, longitudinal-acoustic, and transverse-acoustic phonons, respectively. In addition, we get $\omega_{q\lambda} = c_\lambda q$ for $\lambda = \text{LA and TA}$ by applying the Debye model²⁴ for low-energy acoustic phonons and set $x = \hbar c_\lambda q$ in the second term of Eq. (19). Using the Fröhlich model,²⁴ we find the coupling matrix element between the charged carriers and the LO phonons in Eq. (19)

$$|C_{q,\text{LO}}|^2 = \left(\frac{\hbar \omega_{\text{LO}}}{2} \right) \left(\frac{1}{\epsilon_\infty} - \frac{1}{\epsilon_s} \right) \frac{e^2}{\epsilon_0 (q^2 + q_s^2)}, \quad (20)$$

where $\hbar \omega_{\text{LO}}$ is the energy of LO phonons and ϵ_∞ (ϵ_s) is the high-frequency (static) dielectric constant of the host semiconductor. For the acoustic-phonon scattering in Eq. (19), on the other hand, we use the deformation-potential approximation.²⁴ This yields

$$|C_{q,\text{LA}}|^2 = \left(\frac{\hbar q}{2\rho_0 c_{\text{LA}}} \right) \left[D^2 + \frac{9}{32q^2} (eh_{14})^2 \right] \left(\frac{q^2}{q^2 + q_s^2} \right)^2, \quad (21)$$

$$|C_{q,\text{TA}}|^2 = \left(\frac{\hbar q}{2\rho_0 c_{\text{TA}}} \right) \frac{13}{32q^2} (eh_{14})^2 \left(\frac{q^2}{q^2 + q_s^2} \right)^2, \quad (22)$$

where c_{LA} and c_{TA} are the sound velocities of LA and TA phonons, ρ_0 is the ion mass density of the host semiconductor, D is the deformation-potential coefficient, and h_{14} is the piezoelectric constant. In our calculations, we rewrite Eq. (21) using $q = x/\hbar c_{\text{LA}}$ for $\lambda = \text{LA}$ and Eq. (22) using $q = x/\hbar c_{\text{TA}}$ for $\lambda = \text{TA}$ corresponding to the notation in the second term of Eq. (19). In addition, we have introduced in Eq. (19) the Debye frequency $\omega_m^\lambda = (6\pi^2 N_a)^{1/3} c_\lambda$ for acoustic phonons and the maximum momentum transfer $\hbar q_m = \sqrt{4\mu_r \hbar \omega_{\text{LO}}}$ for optical phonons, where N_a is the atom number density. The screening effect on the carrier-phonon scattering is included in Eqs. (20)–(22) in the Thomas-Fermi limit. When $T_c > T_L$, we find $\mathcal{W}_{\text{ph}}(T_c, T_L) < 0$ from Eq. (19), indicating the loss of thermal energy from hot charged carriers to cool phonons. For a fixed lattice temperature T_L , the carrier temperature $T_c(t)$ can be found from Eq. (17) at each time t . In this situation, optical carrier cooling (heating) using nonthermal e - h plasmas corresponds to $T_c < T_L$ ($T_c > T_L$) for fixed T_L (Ref. 9).

Using the relation between \mathcal{W}_{sp} and \mathcal{R}_{sp} and the steady-state condition of Eq. (1), we can combine the first two terms on the right-hand side of Eq. (17) into one term

$$\beta_{\text{abs}}(\Omega_L) I_0 - \mathcal{W}_{\text{sp}}(T_c) = \int_0^\infty d\omega \left[\frac{d\mathcal{R}_{\text{sp}}(\omega)}{d\omega} \right] (\hbar \Omega_L - \hbar \omega). \quad (23)$$

Here, the positive $d\mathcal{R}_{\text{sp}}(\omega)/d\omega$ represents the emission spectrum as a function of the energy $\hbar \omega$ of emitted photons.

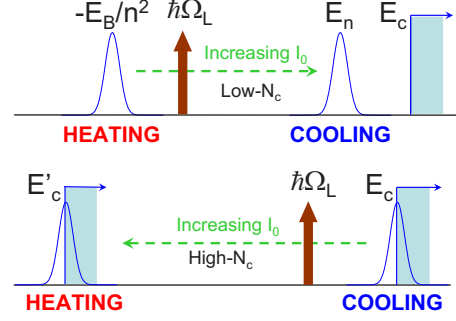


FIG. 1. (Color online) Schematic for the shift of exciton emission peak [solid (blue) curves in the upper panel] in the low-density regime and the shift of e - h plasma emission peak [solid (blue) curves at the conduction-band edge denoted by rectangular (cyan) blocks in the lower panel] in the high-density regime with increasing laser intensity I_0 [horizontal (green) dashed arrows]. In the upper panel, the binding energy of unscreened excitons is $-E_B/n^2$ with $n=1,2,\dots$, while the binding energy of screened excitons is denoted by E_n . In addition, $\hbar\Omega_L$ [upward (brown) arrow] is the fixed laser photon energy. In the lower panel, the unrenormalized conduction-band edge is E_c , while the renormalized conduction-band edge is denoted by E'_c . As explained in the text, a very weak switching from carrier heating to carrier cooling is expected by increasing I_0 when N_c is low in the upper panel, while an opposite strong switching is expected when N_c is high in the lower panel.

In general, the emission spectrum will contain two peaks located at $\hbar\omega = E'_G + E_n$ ($E_n \leq 0$) for excitons and $\hbar\omega = E'_G$ for e - h plasmas. Therefore, if the laser photon energy $\hbar\Omega_L$ is below the emission-peak energy, we expect to see an optical carrier cooling in the system. If the laser photon energy is above the emission-peak energy, on the other hand, we will get an optical carrier heating. As a result, by moving $\hbar\Omega_L$ downward across $E'_G + E_n$, we expect to see the crossover from optical carrier heating to optical carrier cooling, as illustrated in the upper panel of Fig. 1, if the exciton emission dominates when I_0 is low and increases. This is because the exciton binding energy E_n decreases with I_0 or N_c in nonsaturated absorption regime due to a many-body screening effect. In addition, by moving $\hbar\Omega_L$ upward across E'_G , we will find the change from optical carrier cooling to optical carrier heating, as shown in the lower panel of Fig. 1, if the plasma emission dominates when I_0 is high and increases. This is because the band-gap reduction $E_G - E'_G$ increases with I_0 due to the many-body energy renormalization effect. In reality, however, the optical carrier cooling at low I_0 is too weak to be seen since the emission peak in $d\mathcal{R}_{\text{sp}}(\omega)/d\omega$ becomes negligible at very low N_c .

III. NUMERICAL RESULTS AND DISCUSSIONS

In our numerical calculations, we have chosen GaAs as the host semiconductor. The parameters for this host material are listed as follows: $m_e^* = 0.067 m_0$, $m_h^* = 0.62 m_0$, $E_G = 1.519 - 5.405 \times 10^{-4} [T_L^2 / (T_L + 204)] (\text{eV} \cdot \text{K}^{-1})$, $\epsilon_s = 13.18$, $\epsilon_\infty = 10.89$, $\epsilon_b = (\epsilon_s + \epsilon_\infty)/2$, $\hbar\omega_{\text{LO}} = 36.25 \text{ meV}$, $\hbar\omega_{\text{TO}} = 33.29 \text{ meV}$, $c_{\text{LA}} = 5.14 \times 10^5 \text{ cm/s}$, $c_{\text{TA}} = 3.04 \times 10^5 \text{ cm/s}$, $\rho_0 = 5.3 \text{ g/cm}^3$, $D = -9.3 \text{ eV}$, $h_{14} = 1.2 \times 10^7 \text{ V/cm}$, N_a

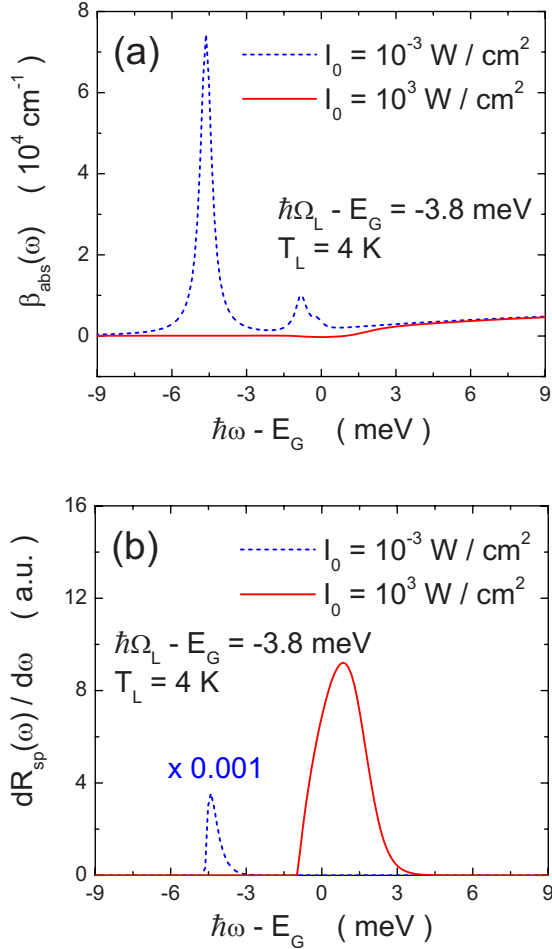


FIG. 2. (Color online) Absorption spectrum $\beta_{\text{abs}}(\omega)$ [in (a) with a unit of 10^4 cm^{-1}] and spontaneous-emission spectrum $dR_{\text{sp}}(\omega)/d\omega$ [in (b) with an arbitrary unit (a.u.)] as functions of the photon energy $\hbar\omega$ with respect to E_G . Here, the dashed (blue) curves correspond to a lower laser intensity $I_0=10^{-3} \text{ W/cm}^2$ ($N_c=3.41 \times 10^{10} \text{ cm}^{-3}$), while the solid (red) curves are associated with a higher laser intensity $I_0=10^3 \text{ W/cm}^2$ ($N_c=9.55 \times 10^{15} \text{ cm}^{-3}$). The label “ $\times 0.001$ ” in (b) indicates that the peak of the dashed (blue) curve has been increased by 10^3 times.

$=4.42 \times 10^{22} \text{ cm}^{-3}$, $\hbar\gamma_0=\hbar\gamma'_0=0.05E_B=0.27 \text{ meV}$, and $T_L=4 \text{ K}$. The above expression for E_G reflects the fact of the reduction of the bare band-gap energy with increasing lattice temperature. The other adjustable parameters such as I_0 and $\hbar\Omega_L$ will be directly given on the figures.

We present in Fig. 2 the calculated steady-state absorption coefficient $\beta_{\text{abs}}(\omega)$ from Eq. (2) [in (a)], as well as the emission spectrum $dR_{\text{sp}}(\omega)/d\omega$ from Eqs. (15) and (16) [in (b)] as a function of the probe photon energy $\hbar\omega-E_G$ at $\hbar\Omega_L-E_G=-3.8 \text{ meV}$ for $I_0=10^{-3} \text{ W/cm}^2$ (blue curves) and $I_0=10^3 \text{ W/cm}^2$ (red curves), respectively. From Fig. 2(a) at $I_0=10^{-3} \text{ W/cm}^2$, we see a very strong absorption peak from the $n=1$ exciton state below the conduction-band edge, as predicted by Eq. (11), in addition to another two weak absorption peaks from $n=2$ and $n=3$ exciton states. However, the step feature in $\beta_{\text{abs}}(\omega)$ due to absorption by e - h plasmas, as predicted by Eq. (4), at the conduction-band edge is almost unresolved in this case. When the incident laser inten-

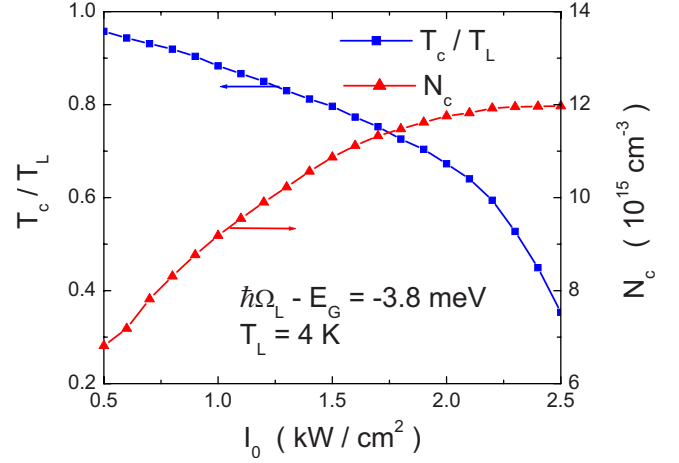


FIG. 3. (Color online) Ratio of the calculated carrier temperature T_c to the fixed lattice temperature T_L [squares (blue) curve and in a left scale] and the calculated density of photocarriers [triangles (red) curve and in a right scale with a unit of 10^{15} cm^{-3}] as functions of the laser intensity I_0 (with a unit of W/cm^2) at $T_L=4 \text{ K}$ for $\hbar\Omega_L-E_G=-3.8 \text{ meV}$.

sity I_0 is high, a large density of photoexcited carriers effectively screens the exciton attractive interaction, as predicted in Eq. (14) with a large value for q_s . As a result, the exciton binding energy becomes negligibly small. At the same time, the ratio of the dipole moments for interband transitions in Eq. (13) is also greatly suppressed. These two factors combined together are responsible for the disappearance of the exciton absorption peaks at $I_0=10^3 \text{ W/cm}^2$. In this case, however, the step feature in $\beta_{\text{abs}}(\omega)$ at the conduction-band edge is enhanced due to the suppressed background from the exciton absorption peaks. The exciton and plasma effects can also be seen from the emission spectrum in Fig. 2(b). For $I_0=10^{-3} \text{ W/cm}^2$, a weak emission peak occurs below the conduction-band edge for the $n=1$ exciton state, which is replaced by a strong peak from the e - h plasmas at the conduction-band edge when $I_0=10^3 \text{ W/cm}^2$. Moreover, the peak value in $dR_{\text{sp}}(\omega)/d\omega$ is found to decrease with T_c .

Figure 3 displays the calculated steady-state carrier temperature T_c/T_L (blue curve) and density N_c of photoexcited carriers (red curve) as functions of the incident laser intensity I_0 for $\hbar\Omega_L-E_G=-3.8 \text{ meV}$. In this case, the laser pumping is set under the conduction-band edge since $\hbar\Omega_L < E_G$, and the exciton effect is negligible for the values of I_0 in the shown range. When I_0 is increased above 2 kW/cm^2 , we find that N_c determined from Eq. (1) becomes nearly independent of I_0 due to saturated optical absorption.³ At the same time, however, T_c/T_L determined from Eq. (17) still drops as I_0 increases, indicating optical carrier cooling due to $T_c/T_L < 1$ in contrast to electrical carrier cooling.⁵ The increasing N_c with I_0 will shrink the band gap from E_G to E'_G determined by Eq. (7), where the renormalized conduction-band edge E'_G roughly labels the peak energy in emission spectrum $dR_{\text{sp}}(\omega)/d\omega$. It is evident that T_c/T_L will eventually increase with I_0 due to optical carrier heating after passing through a minimum, as predicted by Eqs. (17) and (23), similar to electrical carrier heating.⁵

We show in Fig. 4 the calculated steady-state carrier temperature T_c/T_L (blue curve) and peak energy $\hbar\omega_{\text{pl}}-E_G$ of

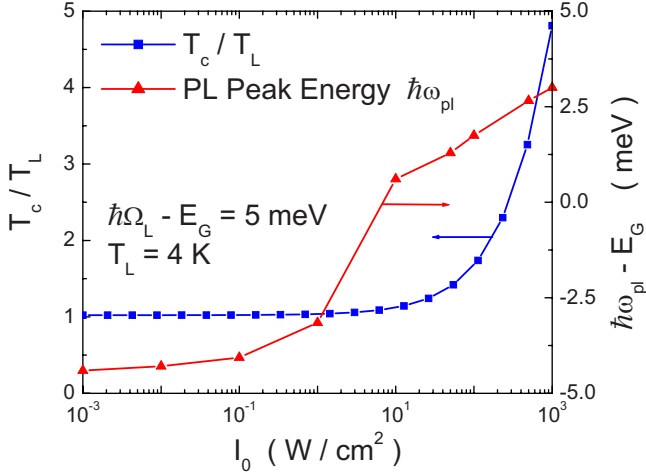


FIG. 4. (Color online) Ratio of the calculated carrier temperature T_c to the fixed lattice temperature T_L [squares (blue) curve and in a left scale] and the peak energy $\hbar\omega_{pl} - E_G$ of emission spectrum with respect to the bare band-gap energy E_G [triangles (red) curve and in a right scale with a unit of meV] as functions of the laser intensity I_0 (with a unit of W/cm^2 and a logarithmic scale) at $T_L = 4 \text{ K}$ for $\hbar\Omega_L - E_G = -3.8 \text{ meV}$.

photoluminescence (red curve) as functions of the incident laser intensity I_0 for $\hbar\Omega_L - E_G = 5 \text{ meV}$ (the laser pumping energy is set above the conduction-band edge due to $\hbar\Omega_L - E_G > 0$). When I_0 is increased up to $1 \text{ W}/\text{cm}^2$, the exciton effect dominates in this range of I_0 . Therefore, $\hbar\omega_{pl} - E_G$ shifts up from -4.4 to -3.2 meV due to the screening effect on the exciton binding energy. When I_0 is increased from $10 \text{ W}/\text{cm}^2$, the emission process will be dominated by e - h plasmas. In this case, $\hbar\omega_{pl} - E_G$ scales with the Fermi edge of e - h plasmas, which moves up in energy with N_c or equivalently with I_0 . When I_0 changes between 1 and $10 \text{ W}/\text{cm}^2$, the emission process switches from exciton dominance to e - h plasma dominance in this crossover region. Correspondingly, T_c/T_L remains unity before the e - h plasma dominance begins. However, T_c/T_L increases dramatically with I_0 once the emission process is dominated by e - h plasmas, indicating a strong optical carrier heating in the system.

Figure 5 exhibits the calculated steady-state temperature difference $T_c - T_L$ (blue curve) and density N_c of photoexcited carriers (red curve) as functions of the frequency detuning $\hbar\Omega_L - E_G$ of a pump laser at $I_0 = 5 \text{ kW}/\text{cm}^2$. For such a large value of I_0 , the e - h plasmas fully dominate the optical process. In the range of $\hbar\Omega_L > E_G$, N_c increases with the frequency detuning in a superlinear dependence since the Fermi energy is proportional to the frequency detuning due to suppressed saturation for optical absorption. On the other hand, in the opposite range of $\hbar\Omega_L < E_G$, N_c decreases with the frequency detuning due to the enhanced peak value in $dR_{sp}(\omega)/d\omega$, and it reaches a minimum slightly below the band gap E_G . Moreover, T_c increases with the frequency detuning from below T_L in the range of $\hbar\Omega_L - E_G < 0$ when $\hbar\Omega_L$ approaches the emission-peak energy around the conduction-band edge, as can be seen from Eq. (23). Once $\hbar\Omega_L > E_G$ is reached, T_c is initially locked to T_L and becomes independent of the frequency detuning due to saturated opti-

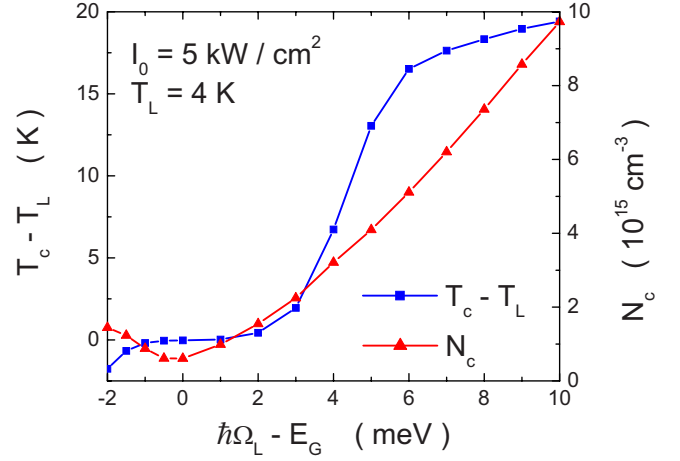


FIG. 5. (Color online) Difference of the calculated carrier temperature T_c and the fixed lattice temperature T_L [squares (blue) curve and in a left scale with a unit of K] and the calculated density of photocarriers [triangles (red) curve and in a right scale with a unit of 10^{15} cm^{-3}] as functions of the detuning of laser photon energy $\hbar\Omega_L - E_G$ with respect to the bare band-gap energy E_G (with a unit of meV) at $T_L = 4 \text{ K}$ for $I_0 = 5 \text{ kW}/\text{cm}^2$.

cal absorption. This is followed by a very strong increase in T_c with the frequency detuning due to enhanced optical absorption after the saturation is suppressed. Finally, the increase in T_c is greatly slowed down due to a reduced peak value in $dR_{sp}(\omega)/d\omega$ with increasing T_c . This demonstrates a switching from optical carrier cooling to heating when the frequency detuning of a pump laser sweeps from below the band gap to above the band gap.

IV. CONCLUSION

In conclusion, we have applied the dynamical density and energy equations to study the steady-state optical carrier cooling in intrinsic semiconductors mediated by nonthermal electron-hole plasmas, where the lattice system is assumed in thermal contact with an external heat bath. We have included many-body effects such as Coulomb renormalization of band-gap energy, screening, and excitonic interaction in the calculations of optical absorption, spontaneous-emission and carrier-phonon scattering. We have demonstrated and explained the many-body effects on optical carrier cooling in the system at low lattice temperatures and studied the dependence of optical carrier cooling on the pump-laser intensity and photon energy.

Auger recombination has not been included in our calculations for low lattice temperatures and low photocarrier densities. We would like to point out that in the current case, the weak Auger recombination in our system is expected to cause a slight modification to the steady-state photocarrier density determined from Eq. (1) and a heating of the lattice through a multiphonon emission process. The modification of the photocarrier density will not alter the predicted many-body effects on optical carrier cooling qualitatively. In addition, the heat dissipated to the lattice by a left-over high-energy excited-state carrier in a weak Auger recombination

process will be completely absorbed by the external heat bath to maintain a fixed lattice temperature.

With a similar procedure used by Rupper *et al.*,¹² we will calculate the following ratio to characterize the importance of the Auger recombination with respect to the radiative recombination, which is given by

$$\frac{C(T)N_c^3}{B(T)N_c^2} = \frac{C(300 \text{ K})}{B(T)} \exp \left[2.24 \left(1 - \frac{300}{T(K)} \right) \right] N_c (\text{cm}^{-3}),$$

where $C(300 \text{ K}) = 4 \times 10^{-30} \text{ cm}^6/\text{s}$ is the room-temperature

Auger-recombination coefficient and $B(T)$ is the radiative-recombination coefficient at the temperature T . Using $T = 10 \text{ K}$, $N_c = 10^{16} \text{ cm}^{-3}$, and $B(10 \text{ K}) = 3 \times 10^{-4} \text{ cm}^3/\text{s}$, we find $[C(10 \text{ K})N_c/B(10 \text{ K})] \ll 1$, which justifies neglecting the Auger recombination in this paper.

ACKNOWLEDGMENTS

This research was supported by the Air Force Office of Scientific Research (AFOSR).

-
- ¹Y. R. Shen, *The Principles of Nonlinear Optics* (Wiley, New York, 1984).
 - ²J. P. Löwenau, S. Schmitt-Rink, and H. Haug, Phys. Rev. Lett. **49**, 1511 (1982).
 - ³H. Haug and S. Schmitt-Rink, J. Opt. Soc. Am. B **2**, 1135 (1985).
 - ⁴H. Haug and S. Schmitt-Rink, Prog. Quantum Electron. **9**, 3 (1984).
 - ⁵X. L. Lei and C. S. Ting, Phys. Rev. B **32**, 1112 (1985).
 - ⁶H. L. Edwards, Q. Niu, G. A. Georgakis, and A. L. de Lozanne, Phys. Rev. B **52**, 5714 (1995).
 - ⁷D. H. Huang, T. Apostolova, P. M. Alsing, and D. A. Cardimona, Phys. Rev. B **70**, 033203 (2004).
 - ⁸T. Apostolova, D. H. Huang, P. M. Alsing, and D. A. Cardimona, Phys. Rev. A **71**, 013810 (2005).
 - ⁹D. H. Huang, T. Apostolova, P. M. Alsing, and D. A. Cardimona, J. Appl. Phys. **98**, 063516 (2005).
 - ¹⁰D. H. Huang, T. Apostolova, P. M. Alsing, and D. A. Cardimona, Phys. Rev. B **72**, 195308 (2005).
 - ¹¹J. Hader, J. V. Moloney, and S. W. Koch, IEEE J. Quantum Electron. **41**, 1217 (2005).
 - ¹²G. Rupper, N. H. Kwong, and R. Binder, Phys. Rev. B **76**, 245203 (2007).
 - ¹³M. Sheik-Bahae and R. I. Epstein, Phys. Rev. Lett. **92**, 247403 (2004).
 - ¹⁴M. Lindberg and S. W. Koch, Phys. Rev. B **38**, 3342 (1988); J. V. Moloney, R. A. Indik, J. Hader, and S. W. Koch, J. Opt. Soc. Am. B **16**, 2023 (1999).
 - ¹⁵J. Li and C. Z. Ning, Phys. Rev. A **66**, 023802 (2002).
 - ¹⁶W. Shockley and W. T. Read, Jr., Phys. Rev. **87**, 835 (1952).
 - ¹⁷D. H. Huang, Phys. Rev. B **53**, 13645 (1996).
 - ¹⁸S. Das Sarma and J. J. Quinn, Phys. Rev. B **25**, 7603 (1982).
 - ¹⁹P. C. Martin and J. Schwinger, Phys. Rev. **115**, 1342 (1959).
 - ²⁰W. Hoyer, C. Ell, M. Kira, S. W. Koch, S. Chatterjee, S. Mosor, G. Khitrova, H. M. Gibbs, and H. Stolz, Phys. Rev. B **72**, 075324 (2005).
 - ²¹C. H. Henry, R. A. Logan, and F. R. Merritt, J. Appl. Phys. **51**, 3042 (1980).
 - ²²D. H. Huang and S. K. Lyo, Phys. Rev. B **59**, 7600 (1999).
 - ²³S. K. Lyo and E. D. Jones, Phys. Rev. B **38**, 4113 (1988).
 - ²⁴J. M. Ziman, *Principles of the Theory of Solids*, 1st ed. (Cambridge University Press, Cambridge, England, 1964).